Journal of Nuclear Medicine, published on April 26, 2018 as doi:10.2967/jnumed.118.208744

Title: Imaging melphalan therapy response in preclinical extramedullary myeloma with ^{18}F-FDOPA and ^{18}F-FDG PET

Authors: Deep K Hathi[1,2], Elizabeth N DeLassus[3], Samuel Achilefu[1,2,3], Jonathan McConathy[4], Monica Shokeen[1,2*]

Affiliation: (1) Washington University in St. Louis, Department of Biomedical Engineering; (2) Washington University in St. Louis, Department of Radiology; (3) Washington University in St. Louis, Department of Biochemistry and Biophysics; (4) University of Alabama in Birmingham, Department of Radiology

Disclaimer: None

Financial Support: This research was primarily funded by the R01 CA176221 and U54 CA199092. We acknowledge the support from P50 CA094056, P30 CA091842, DE-SC0012737, K08CA154790, and the MIR pilot imaging funds.

Corresponding author: Monica Shokeen, 4515 McKinley Ave RM 2216, St. Louis, MO 63110, 314-362-8979, mshokeen@wustl.edu

First author: Deep K Hathi, 4515 McKinley Ave RM 2213, St. Louis, MO 63110, 314-747-0588, deep.hathi@wustl.edu, Student

Word count: 4910

Running title: Imaging melphalan therapy response

ABSTRACT

Multiple myeloma (MM) is a debilitating neoplasm of terminally differentiated plasma B-cells that has resulted in over 13,000 deaths in 2017 alone. Combination therapies involving melphalan, a small molecule DNA alkylating agent, are commonly prescribed to patients with relapsed/refractory MM, which necessitates the stratification of responding patients to minimize toxicities and improve quality of life. Here, we evaluated the use of ^{18}F-FDOPA, a clinically available positron emission tomography (PET) radiotracer with specificity to the L-type amino acid transporter-1 (LAT1), which also mediates melphalan uptake, for imaging melphalan therapy response in a preclinical immunocompetent model of MM.

Methods: C57Bl/KaLwRij mice were implanted subcutaneously with unilateral murine 5TGM1-GFP tumors, and divided into three independent groups: untreated, treated beginning week 2, and treated beginning week 3 post tumor implantation. The untreated and week 2 therapy cohorts were imaged with preclinical magnetic resonance imaging (MRI) and dynamic ^{18}F-FDG and ^{18}F-FDOPA-PET/computed tomography (PET/CT) at week 4 on separate, contiguous days, while the week 3 therapy cohort was longitudinally imaged weekly for 2 weeks. Metabolic tumor volume, lesion avidity, maximum standard uptake value, and total uptake metrics were calculated for both tracers. Immunohistochemistry was performed on representative tissue from all groups for LAT1 and glucose transporter-1 (GLUT1) expression.

Results: Melphalan therapy induced a statistically significant reduction in lesion avidity and uptake metrics for both ^{18}F-FDG and ^{18}F-FDOPA. There was no visible effect on GLUT1 expression, but LAT1 density was increased in the week 2 therapy cohort. Longitudinal imaging of the week 3 group showed variable changes in ^{18}F-FDG and ^{18}F-FDOPA uptake, with increase in ^{18}F-FDOPA lesion avidity in the 2nd week relative to baseline. LAT1 and GLUT1 surface density in the untreated tumor and week 3 treatment group were qualitatively similar.

Conclusion: ^{18}F-FDOPA-PET/CT served as a complementary method to ^{18}F-FDG-PET/CT in imaging melphalan therapy response in extramedullary preclinical MM. ^{18}F-FDOPA uptake was linked to LAT1 expression and melphalan response, with longitudinal imaging suggesting stabilization of LAT1 levels and melphalan tumor cytotoxicity. Future work will explore additional MM cell lines with heterogeneous LAT1 expression and response to melphalan therapy.

KEYWORDS: ^{18}F-FDOPA-PET, ^{18}F-FDG-PET, Melphalan therapy response, Multiple myeloma

INTRODUCTION

Multiple myeloma (MM) is a cancer of terminally differentiated plasma B-cells that originates in the hematopoietic bone marrow and accounts for 15-20% of all hematologic malignancies(*1,2*). In the last decade, the availability of autologous stem cell transplantation and combination therapies consisting of immunomodulatory drugs, proteasome inhibitors, and other chemotherapeutics has improved median 5-year survival from 34.6% in 2004 to 49.6% in 2013(*3,4*). One of the main therapies used for treating MM is the small molecule alkylating agent melphalan(*5-7*). However, melphalan efficacy is variable in the clinical population, especially in relapsed and refractory MM. It is also implicated in various toxicities including severe mucositis and myelosuppression. Thus, stratification of melphalan-responsive patients in the MM patient population is critical for reducing therapy-induced toxicities.

The L-type amino acid transporter-1 (LAT1) is a key mediator in the uptake and intracellular accumulation of melphalan and is correlated to melphalan sensitivity and response in MM and other cancers(*8-10*). LAT1 (SLC7A5) is a member of the system L family of transporters and is primarily expressed in fetal liver, bone marrow, placenta, and testes(*11,12*). It is overexpressed in MM and correlated to poor myeloma prognosis and survival(*10*). LAT1 is a heterodimer consisting of a light chain (SLC7A5), which provides the amino acid transporter function, and a glycosylated heavy chain subunit (CD98), which provides trafficking and membrane localization(*13,14*). LAT1 is implicated in tumor proliferation pathways, through the mammalian target of rapamycin and glutamine/glutamate signaling pathways(*15*).

The glucose analog 2-deoxy-2-[^{18}F]-fluorodeoxyglucose (^{18}F-FDG) is currently used for positron emission tomography (PET) imaging of myeloma and other cancers for disease staging and monitoring therapy response. Clinical trials in patients with MM have correlated the suppression of ^{18}F-FDG uptake to improved event-free survival(*16*). ^{18}F-FDG-PET/CT is useful for staging and response monitoring in MM, but the sensitivity for detecting marrow involvement by MM is variable, particularly with relatively low marrow burden of disease(*17*). ^{18}F-FDG uptake can be increased in the setting of inflammation after chemotherapy and in the presence of exogenous or endogenous marrow stimulation. Thus, there is a need for other PET tracers with increased sensitivity and specificity for detecting intramedullary myeloma, particularly for low disease burden. Additionally, ^{18}F-FDG uptake and retention is mediated by glucose transporter-1 (GLUT1) and hexokinase, which are involved primarily in glycolysis. As a result, ^{18}F-FDG uptake does not report on LAT1 expression and the melphalan sensitivity of MM tumors.

In this study, we sought an alternative tracer that directly interrogates the functional status of LAT1. The amino acid PET tracer 3,4-dihydroxy-6-[^{18}F]fluoro-L-phenylalanine (^{18}F-FDOPA) is structurally related to melphalan and is primarily transported into cells by LAT1(*18*). ^{18}F-FDOPA-PET is mostly used in imaging gliomas and neuroendocrine tumors in cancer patients(*19,20*). Because LAT1 mediates the intracellular accumulation of both ^{18}F-FDOPA and melphalan, we hypothesized that the quantification of ^{18}F-FDOPA uptake in myeloma cells will correlate with melphalan therapy response. Using an immunocompetent xenograft model of murine myeloma, we demonstrate that ^{18}F-FDOPA could serve as a complementary imaging agent to ^{18}F-FDG for MM PET imaging and potentially provide additional stratification of responders and non-responders to melphalan therapy.

MATERIALS AND METHODS

Cell Culture and Reagents

5TGM1-GFP (5TGM1) (originally a kind gift from Dr. G. Mundy, Vanderbilt University, TN, USA; 5TGM1-GFP cells were obtained from Dr. Katherine N. Weilbaecher, Washington University, Department of Medicine) were maintained at 10^6 cells/mL in Iscove's Modified Dulbecco Medium supplemented with 10% v/v fetal bovine serum and 1% penicillin/streptomycin (all from Thermo Fisher Scientific, MA, USA). Melphalan (Sigma Aldrich, MO, USA) was prepared prior to weekly injections from 5 mg/mL 0.1M HCl EtOH stock. ^{18}F-FDG and ^{18}F-FDOPA were produced in compliance with current good manufacturing practices by the Washington University Cyclotron Facility.

Tumor Model and Melphalan Therapy

All animal studies were conducted according to protocols approved by the Washington University Animal Studies Committee. C57Bl/6 KaLwRij mice were unilaterally injected subcutaneously in the lower flank region with 10^6 5TGM1 cells. All tumor implantation and imaging procedures were conducted under 1-2% v/v isoflurane/100% O_2 anesthesia.

Tumor-bearing mice were separated into two independent studies. The first group consisted of two independent cohorts of treated (n=7) and untreated (n=6) mice, with melphalan therapy beginning at 14-18 days after tumor implantation. Imaging was performed at week 4 (**Fig. 1A**). The second group (n=3) consisted of mice treated with melphalan beginning week 3 after tumor implantation. Imaging was performed weekly immediately prior to the start of the therapy regimen and continued until week 5 (**Fig. 1B**). Melphalan therapy was administered weekly at 10mg/kg intraperitoneally in saline in each of the studies(*21*).

In Vivo Structural and Metabolic Imaging

Prior to PET/CT imaging, tumor structural volume was assessed by calipers and small animal magnetic resonance imaging (MRI). Mice were placed supine within a birdcage radiofrequency coil and imaged in 4.7 T (200 MHz) Varian/Agilent small animal scanner (Agilent Technologies, CA, USA). Respiration and body temperature were maintained at approximately 50 breaths/minute and 37 ^{o}C, respectively. Transverse T_2-weighted contiguous slices were collected using a spin echo sequence (repetition time, 1.5s; echo time, 40ms; averages, 2; field of view, 2.5 x 2.5 x 1.6 cm^3; data matrix 128 x 128 x 16). Region of interest analysis was performed using ImageJ (National Institutes of Health, MD, USA).

^{18}F-FDG and ^{18}F-FDOPA-PET/CT were performed on separate, contiguous days to minimize signal cross-contamination. Prior to radiotracer administration, a whole-body 60kVp CT was acquired on each mouse. Mice were injected intravenously with 7.4 MBq dosage of the tracer *via* the lateral tail vein. 60-minute dynamic scans were collected following injection of the tracer using Inveon PET/CT or Focus F220 PET imaging systems (all from Siemens Healthcare, Erlangen, Germany). ^{18}F-FDG-PET/CT was performed after mice were fasted for 6-8 hours with access to water. To standardize imaging, ^{18}F-FDOPA-PET/CT was performed after ^{18}F-FDG-PET/CT. ^{18}F-FDG and ^{18}F-FDOPA-PET/CT images were reconstructed using iterative reconstruction and displayed using Inveon Research Workplace 4.2 (Siemens Healthcare) in multi-planar views.

PET Image Analysis

Volumetric tumor and control tissue regions of interest were defined using companion CT and summed PET. Dynamic time activity curves (TACs) were decay corrected and converted to standard uptake values (SUV) prior to analysis. The metabolic tumor volume (MTV) (volume of tumor with $SUV > 0.42*SUV_{Max}$)(*22*), total lesion avidity (TLA) (Mean SUV in the MTV ($SUV_{Mean, MTV}$) * MTV), and total uptake (area under the curve of tracer TAC) were calculated for ^{18}F-FDOPA. MTV, total lesion glycolysis (TLG) ($SUV_{Mean, MTV}$ * MTV), and total uptake were also measured for ^{18}F-FDG. To minimize single voxel noise in SUV_{Max} measurements, SUV_{Max} was defined as the mean of the 95% isocontour(*23*).

Immunohistochemistry

Tumor tissue was excised, flash frozen in optimal cutting temperature compound (Tissue Tek, CA, USA), and stored at -20 ^{o}C. Tyramide amplified immunohistochemistry using Perkin Elmer TSA-Cy3 kit (PerkinElmer, Inc., MA, USA) was performed as per manufacturer’s protocol(*24*). Briefly, sections were fixed in 4% v/v paraformaldehyde/phosphate buffered saline.

Endogenous peroxidase and non-specific binding was blocked with 3% H_2O_2 and 0.5% TSA blocking reagent, respectively. Sections were incubated separately overnight at 4 ^oC with 1:50 dilutions of rabbit polyclonal anti-SLC7A5 (Proteintech Group, Inc., IL, USA), anti-GLUT1 (Abcam, Cambridge, UK), anti-CD98 (Santa Cruz Biotechnology, Inc., TX, USA), and anti-CD31 (Novus Biologicals, Littleton, CO, USA). The slides were mounted with Vectashield anti-fade mounting medium with DAPI (Vector Laboratories, Inc., CA, USA) after signal amplification with 1:50 TSA-Cy3. Stained slides were imaged on a Zeiss LSM 880 II Airyscan inverted confocal fluorescence microscope (Zeiss, Oberkochen, Germany). Slides were sequentially imaged with DAPI (excitation/emission 405/465 nm), GFP (excitation/emission 488/509 nm), and Cy3 (excitation/emission 561/603 nm) filters. As a negative control, muscle tissue excised from the contralateral leg was stained and imaged using the described settings.

Statistical Analysis

All statistical analysis was performed using GraphPad Prism 5.0 (GraphPad, CA, USA). Statistical significance between TACs was determined using 2-way analysis of variance (ANOVA) with repeated measures, while 1-way ANOVA with Bonferroni multiple comparisons post-testing and Student's two-tailed *t*-test were used for avidity, uptake, and volume comparisons between tracers, treatment, and tissue types. Lin's concordance correlation coefficients between ^{18}F-FDOPA and ^{18}F-FDG parameters were calculated using MATLAB 2014b (Mathworks, Inc., MA, USA).

RESULTS

C57Bl/KaLwRij mice implanted subcutaneously with 5TGM1 congenic unilateral flank tumors were evaluated for ^{18}F-FDG and ^{18}F-FDOPA uptake at four weeks post tumor injection with 60 min dynamic PET/CT. Structural tumor volume was assessed with T_2-weighted non-contrast enhanced MRI. There was heterogeneous structural tumor volume reduction from melphalan therapy within the treatment cohort (9.9 ± 7.7-fold) (**Table 1; Fig. 2A-B**). Correspondingly, metabolic volume representing ^{18}F-FDG and ^{18}F-FDOPA uptake decreased in treated mice relative to untreated mice (**Fig. 3A-B**). Decay-corrected dynamic TACs derived from the tumor volume of interest for ^{18}F-FDG and ^{18}F-FDOPA showed decreased overall uptake across imaging time for treated mice (**Fig. 3C-D**). Interestingly, treatment did not affect time to steady state in ^{18}F-FDOPA TACs, suggesting that melphalan therapy did not impact the overall uptake mechanism and washout kinetics in the tumors.

Avidity and uptake of both ^{18}F-FDOPA and ^{18}F-FDG were reduced in the treated tumors. There was a larger reduction in ^{18}F-FDOPA MTV (28.7 ± 13.2-fold) than ^{18}F-FDG MTV (14.4 ± 6.9-fold), although this difference in MTV reduction did not translate to significant correlation between MTV and structural tumor volume. Reductions in TLA and TLG were similar in treated tumors (**Fig. 4A**). Overall ^{18}F-FDG SUV_{max} was higher in both untreated and treated tumors than ^{18}F-FDOPA SUV_{max} untreated and treated tumors (**Fig. 4B; Table 1**). ^{18}F-FDOPA total uptake and maximal uptake metrics fell within control tissue levels upon melphalan treatment, as measured relative to bone marrow and muscle, while ^{18}F-FDG uptake remained significantly higher relative to control tissue within the tumor (**Fig. 4C**). These results suggest that changes in ^{18}F-FDOPA uptake may be more specific to melphalan-mediated reduction in tumor size than ^{18}F-FDG for this tumor model.

^{18}F-FDOPA measurements were also assessed against ^{18}F-FDG using Lin's concordance correlation coefficients. Avidity and MTV in the treated cohort were moderately concordant, while SUV_{Max} and total tracer uptake demonstrated poor agreement (**Table 2**). Interestingly, ^{18}F-FDOPA TLA and total uptake were correlated more strongly post therapy to ^{18}F-FDG, while the concordance of MTV and SUV_{max} between ^{18}F-FDOPA and ^{18}F-FDG was relatively unaffected. The lack of concordance between ^{18}F-FDOPA and ^{18}F-FDG in the SUV_{Max} and total uptake is likely linked to the difference in uptake mechanisms, while moderate agreement between MTV and avidity indicated similar global effects on metabolism in the setting of effective therapy.

We next performed weekly ^{18}F-FDOPA and ^{18}F-FDG-PET/CT and MRI to study the effect of therapy on established tumors (**Fig. 1B**). T_2-weighted MRI indicated minimal structural tumor volume reduction throughout the therapy regimen (**Fig. 2C**). ^{18}F-FDG uptake was significantly reduced in week 1 of therapy, with a return to pretreatment levels during week 2 (**Fig. 5A; Supplemental Fig. 1A**). TLG (1.7 ± 0.4-fold), SUV_{Max} (2.1 ± 0.4-fold), and total ^{18}F-FDG uptake (2.1 ± 0.4-fold) also increased by week 2 of therapy, suggesting a rebound of glucose-avid tumor cells (**Supplemental Fig. 1B-D**). By contrast, ^{18}F-FDOPA kinetics were unaffected by the therapy regimen (**Fig. 5B; Supplemental Fig. 1A**). There was an increase in TLA (2.4 ± 0.9-fold) between the pretreatment baseline and week 1, which remained consistent at week 2 (0.8 ± 0.2-fold relative to week 1) (**Supplemental Fig. 1B**). There was no corresponding change in SUV_{Max} or total ^{18}F-FDOPA uptake (**Supplemental Fig. 1C-D**). These results suggested that treatment of established tumors with melphalan may result in the stabilization of the structural and metabolic tumor volumes. Additionally, the lack of correlation between ^{18}F-FDOPA and ^{18}F-FDG uptake indicated that acute changes in glucose metabolism are independent of changes in the transport and intracellular metabolism of the amino acid ^{18}F-FDOPA.

Immunohistochemistry was performed on tissue from both treatment groups to evaluate changes in LAT1 and GLUT1 transporter expression. Changes in LAT1 expression were modulated by both tumor size and therapy. Mice in the melphalan-treated established tumor cohort (week 3 treatment group) had reduced LAT1 (**Fig. 6C top**) surface density relative to the treatment regimen started week 2 post tumor implantation (week 2 treatment group) and the untreated tumor (**Fig. 6A-B top**). The high LAT1 density in the week 2 treatment group relative to the untreated tumors could be attributed to the smaller tumor size and increased tumor vascular density. Indeed, LAT1 and GLUT1 expression was generally concentrated near blood vessels, as confirmed by CD31 staining (**Supplemental Fig. 2A-B top**). The relative lack of LAT1 signal in the untreated tumor may be linked to the heterogeneous distribution of viable GFP-expressing tumor cells within the tumor mass.

DISCUSSION

^{18}F-FDOPA is an aromatic amino acid PET tracer that is effective for imaging gliomas and neuroendocrine tumors(*19,20*). Dimitrakopoulou-Strauss *et al* showed that ^{18}F-FDOPA and ^{18}F-FDG uptake provided complementary detection of metastatic melanoma in pretreated patients(*25*). ^{18}F-FDOPA uptake by cancer cells is thought to be primarily mediated by LAT1, making it a promising candidate for imaging LAT1 activity *in vivo*. Since melphalan uptake is also mediated by LAT1, we used ^{18}F-FDOPA-PET as a surrogate reporter of melphalan therapy efficacy in a preclinical, immunocompetent MM model. We evaluated ^{18}F-FDOPA and ^{18}F-FDG uptake parameters, including TLA, MTV, and SUV_{Max} *in vivo* in unilateral subcutaneously implanted 5TGM1 tumors in C57Bl/KaLwRij mice, which served as a model for extramedullary myeloma. Importantly, uptake of ^{18}F-FDOPA correlated strongly to LAT1 surface expression and showed a significant therapy-induced decrease in SUV_{Max}, lesion avidity, and total uptake relative to untreated tumor.

Preclinical ^{18}F-FDOPA-PET/CT showed demonstrably different tumor uptake in the untreated and the two therapy groups. Immunohistochemistry of the week 2 treatment group suggested that decreasing tumor sizes and increased viable tumor fraction were linked to increased LAT1 expression (**Fig. 6A-B top**). To further validate changes in expression of LAT1, CD98 staining was performed. It should be noted, however, that CD98 also forms heterodimers with other amino acid transporters, including members of the LAT family(*14*). Additionally, CD98 expression is implicated in increased vascular density (**Supplemental Fig. 2A-B bottom**)(*26*). The correlation between vascular density and LAT1 expression is corroborated by ^{11}Cmethionine preclinical PET studies of gliomas and brain tumors(*27*). ^{18}F-FDOPA metrics also correlated with melphalan sensitivity, with moderate concordance in MTV to the ^{18}F-FDG-PET clinical reference standard (**Table 2**). The reduction in ^{18}F-FDOPA uptake indicated the sensitivity of ^{18}F-FDOPA-PET/CT to melphalan cytotoxicity.

There was a larger effect on total uptake and SUV_{Max} for ^{18}F-FDG in response to aggressive melphalan therapy (**Fig. 4B-C**). The 5TGM1 cell line is highly glucose avid and aggressive relative to several other human and murine myeloma cell lines. This avidity, coupled with minimal GLUT1 surface density differences in untreated and treated tumors, may explain the differences in overall uptake of ^{18}F-FDG relative to ^{18}F-FDOPA in this tumor model. ^{18}F-FDG SUV_{Max} and total uptake was also significantly higher in the treated tumor relative to non-tumor tissue. This effect may be partially explained by the recruitment of glucose avid macrophages and other immune cells to the tumor by therapy-induced inflammation. Nevertheless, ^{18}F-FDG-PET/CT provided accurate identification of overall response, while ^{18}F-FDOPA-PET/CT highlighted melphalan-sensitive tumor populations and showed a greater reduction in MTV in the treatment group compared to the untreated tumors than did ^{18}F-FDG.

The differences in ^{18}F-FDOPA and ^{18}F-FDG uptake induced by the aggressive therapy regimen may be overstated by several factors, including variable tumor viability, immunologic response, and the homogeneous expression of LAT1 in the viable tumor volume. To address these concerns, we performed longitudinal ^{18}F-FDOPA and ^{18}F-FDG-PET/CT on established tumors treated with melphalan (**Fig. 1B**). There was no significant difference in ^{18}F-FDOPA MTV, SUV_{Max}, or total uptake observed during the imaging period (**Fig. 5B; Supplemental Fig. 1**). There was a 2.4-fold increase in TLA between the baseline and first week of therapy, which remained unchanged at the second week (**Supplemental Fig. 1B**). Indeed, immunohistochemistry showed that LAT1 expression in this treatment group did not differ qualitatively from the untreated tumor, which suggests therapy-induced stabilization of LAT1 expression within the tumor environment (**Fig. 6C**). By contrast, ^{18}F-FDG SUV_{Max} and total uptake rebounded to pre-treatment levels after the first week of therapy, indicating reduction in therapy killing effect by the second week and stabilized tumor viability (**Supplemental Fig. 1C-D**). These results suggest that functional imaging with ^{18}F-FDOPA and ^{18}F-FDG PET/CT may be linked to tumor viability and melphalan therapy response.

Use of indirect metabolic markers such as lesion avidity and radiotracer uptake have been established in the literature as potential parameters sensitive to changes in cancer staging. TLA and TLG, while derived from similar SUV data, provided different results from total uptake, due to the selective volumetric information contained within the MTV. TLA is a crucial semi-quantitative parameter that may provide a surrogate measurement for viable tumor fraction. TLG is a more mechanistic measurement that represents the tracer uptake mediated by the glucose transport proteins and the subsequent intracellular trapping of ^{18}F-FDG following phosphorylation by hexokinases. While phosphorylated ^{18}F-FDG is unable to enter glycolysis further downstream, TLG can provide information on the changing GLUT1 mediated metabolism during disease progression and following therapeutic intervention. Indeed, McDonald *et al* have shown that ^{18}F-FDG TLG, MTV, SUV_{Max}, and the number of focal lesions strongly correlated to MM stage and progression-free and overall survival rates(*28*). Similarly, our results highlight the discordance in the changes in TLA and TLG in response to melphalan therapy in the established tumors. Therefore, ^{18}F-FDG and ^{18}F-FDOPA may provide an assessment of tumor response to melphalan during early and late stages, respectively.

This study was a proof of concept investigation into ^{18}F-FDOPA-PET imaging of myeloma and the correlation between ^{18}F-FDOPA to melphalan therapeutic efficacy in an extramedullary myeloma tumor model. There are several promising results from this study, including the correlation between ^{18}F-FDOPA and ^{18}F-FDG uptake with tumor viability and early response to melphalan therapy, respectively. Imaging in other human and murine myeloma cell lines and animal models with different LAT1 expression and melphalan sensitivity would provide additional corroboration for the trends seen within these data. Efflux transporters are predominantly linked to melphalan resistance in *in vitro* studies of melphalan-resistant myeloma cell lines(*29*). Therefore, determining the expression of efflux transporters at various time-points during melphalan therapy would also provide important information about treatment-mediated transient changes in influx and efflux transporters. Finally, further investigation into ^{18}F-FDOPA uptake and washout mechanisms with metabolite fate analyses and competitive inhibition of ^{18}F-FDOPA intracellular uptake can provide the means for developing strong predictive models of melphalan sensitivity with ^{18}F-FDOPA-PET/CT.

CONCLUSION

This study represents, to date, one of the first investigations linking amino acid-based imaging in MM to therapy response, *via* the correlation of ^{18}F-FDOPA-PET/CT to melphalan sensitivity and LAT1 expression. ^{18}F-FDOPA-PET/CT provided viable and complementary imaging of MM and melphalan therapy efficacy in this tumor model. Finally, uptake of ^{18}F-FDG and ^{18}F-FDOPA in established tumors were discordant early after treatment initiation, indicating the tracers' independent mechanisms and their individual applications for assessing response to different stages of melphalan therapy.

ACKNOWLEDGEMENTS

Ms. Gail Sudlow assisted with subcutaneous injections and tissue sectioning. Mr. John Engelbach assisted in the setup and acquisition of MR images. Ms. Wadha Alyami assisted in the preliminary data collection.

REFERENCES

1. Palumbo A, Anderson K. Multiple myeloma. *N Engl J Med.* 2011;364:1046-1060.

2. Becker N. Epidemiology of multiple myeloma. In: Moehler T, Goldschmidt H, eds. *Multiple Myeloma*. Berlin, Heidelberg: Springer Berlin Heidelberg; 2011:25-35.

3. Brenner H, Gondos A, Pulte D. Recent major improvement in long-term survival of younger patients with multiple myeloma. *Blood.* 2008;111:2521-2526.

4. Seer database. https://seer.cancer.gov/statfacts/html/mulmy.html. Accessed December 16, 2017.

5. Palumbo A, Sezer O, Kyle R, et al. International Myeloma Working Group guidelines for the management of multiple myeloma patients ineligible for standard high-dose chemotherapy with autologous stem cell transplantation. *Leukemia.* 2009;23:1716-1730.

6. Waage A, Gimsing P, Fayers P, et al. Melphalan and prednisone plus thalidomide or placebo in elderly patients with multiple myeloma. *Blood.* 2010;116:1405-1412.

7. Facon T, Mary JY, Hulin C, et al. Melphalan and prednisone plus thalidomide versus melphalan and prednisone alone or reduced-intensity autologous stem cell transplantation in elderly patients with multiple myeloma (IFM 99–06): a randomised trial. *Lancet.* 2007;370:1209-1218.

8. Kim DK, Kanai Y, Choi HW, et al. Characterization of the system L amino acid transporter in T24 human bladder carcinoma cells. *Biochim Biophys Acta Biomembr.* 2002;1565:112-122.

9. Lin J, Raoof DA, Thomas DG, et al. l-Type Amino Acid Transporter-1 Overexpression and Melphalan Sensitivity in Barrett's Adenocarcinoma. *Neoplasia.* 2004;6:74-84.

10. Isoda A, Kaira K, Iwashina M, et al. Expression of L-type amino acid transporter 1 (LAT1) as a prognostic and therapeutic indicator in multiple myeloma. *Cancer Sci.* 2014;105:1496-1502.

11. Bhutia YD, Babu E, Ramachandran S, Ganapathy V. Amino Acid transporters in cancer and their relevance to "glutamine addiction": novel targets for the design of a new class of anticancer drugs. *Cancer Res.* 2015;75:1782-1788.

12. Yanagida O, Kanai Y, Chairoungdua A, et al. Human L-type amino acid transporter 1 (LAT1): characterization of function and expression in tumor cell lines. *Biochim Biophys Acta Biomembr.* 2001;1514:291-302.

13. Napolitano L, Scalise M, Galluccio M, Pochini L, Albanese LM, Indiveri C. LAT1 is the transport competent unit of the LAT1/CD98 heterodimeric amino acid transporter. *Int J Biochem Cell Biol.* 2015;67:25-33.

14. Wagner CA, Lang F, Broer S. Function and structure of heterodimeric amino acid transporters. *Am J Physiol Cell Physiol.* 2001;281:C1077-1093.

15. Altman BJ, Stine ZE, Dang CV. From Krebs to clinic: glutamine metabolism to cancer therapy. *Nat Rev Cancer.* 2016;16:749.

16. Agarwal A, Chirindel A, Shah BA, Subramaniam RM. Evolving role of FDG PET/CT in multiple myeloma imaging and management. *Am J Roentgenol.* 2013;200:884-890.

17. Cavo M, Terpos E, Nanni C, et al. Role of 18F-FDG PET/CT in the diagnosis and management of multiple myeloma and other plasma cell disorders: a consensus statement by the International Myeloma Working Group. *The Lancet Oncology.* 2017;18:e206-e217.

18. Youland RS, Kitange GJ, Peterson TE, et al. The role of LAT1 in (18)F-DOPA uptake in malignant gliomas. *J Neurooncol.* 2013;111:11-18.

19. Schwarzenberg J, Czernin J, Cloughesy TF, et al. Treatment response evaluation using 18F-FDOPA PET in patients with recurrent malignant glioma on Bevacizumab therapy. *Clin Cancer Res.* 2014.

20. Becherer A, Szabó M, Karanikas G, et al. Imaging of advanced neuroendocrine tumors with 18F-FDOPA PET. *J Nucl Med.* 2004;45:1161-1167.

21. Mori Y, Shimizu N, Dallas M, et al. Anti-α4 integrin antibody suppresses the development of multiple myeloma and associated osteoclastic osteolysis. *Blood.* 2004;104:2149-2154.

22. Ulaner GA, Goldman DA, Corben A, et al. Prospective clinical trial of (18)F-Fluciclovine PET/CT for determining the response to neoadjuvant therapy in invasive ductal and invasive lobular breast cancers. *J Nucl Med.* 2017;58:1037-1042.

23. Vanderhoek M, Perlman SB, Jeraj R. Impact of the definition of peak standardized uptake value on quantification of treatment response. *J Nucl Med.* 2012;53:4-11.

24. Zaidi AU, Enomoto H, Milbrandt J, Roth KA. Dual Fluorescent In Situ Hybridization and Immunohistochemical Detection with Tyramide Signal Amplification. *J Histochem Cytochem.* 2000;48:1369-1375.

25. Dimitrakopoulou-Strauss A, Strauss LG, Burger C. Quantitative PET studies in pretreated melanoma patients: a comparison of 6-[18F]fluoro-L-dopa with 18F-FDG and (15)O-water using compartment and noncompartment analysis. *J Nucl Med.* 2001;42:248-256.

26. Liao Z, Cantor JM. Endothelial cells require CD98 for efficient angiogenesis-brief report. *Arterioscler Thromb Vasc Biol.* 2016;36:2163-2166.

27. Okubo S, Zhen HN, Kawai N, Nishiyama Y, Haba R, Tamiya T. Correlation of L-methyl-11C-methionine (MET) uptake with L-type amino acid transporter 1 in human gliomas. *J Neurooncol.* 2010;99:217-225.

28. McDonald JE, Kessler MM, Gardner MW, et al. Assessment of total lesion glycolysis by (18)F FDG PET/CT significantly improves prognostic value of GEP and ISS in myeloma. *Clin Cancer Res.* 2017;23:1981-1987.

29. Kuhne A, Tzvetkov MV, Hagos Y, Lage H, Burckhardt G, Brockmoller J. Influx and efflux transport as determinants of melphalan cytotoxicity: Resistance to melphalan in MDR1 overexpressing tumor cell lines. *Biochem Pharmacol.* 2009;78:45-53.

Figures

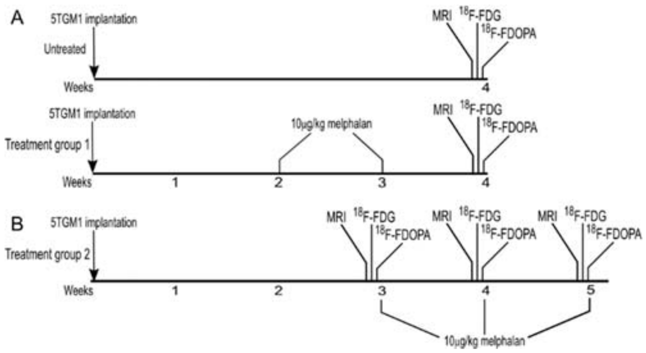

FIGURE 1: Timeline for melphalan treated and untreated cohorts. Melphalan was administered weekly beginning either (A) week 2, with imaging performed on separate, contiguous days at the end of the study, or (B) week 3 post tumor implantation. Longitudinal imaging with MRI, ^{18}F-FDG, and ^{18}F-FDOPA PET/CT was initialized prior to the start of therapy for the week 3 cohort and continued through to week 5 post tumor implantation.

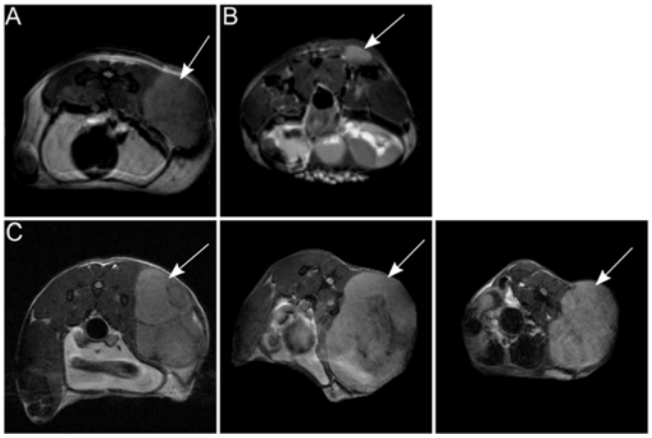

FIGURE 2: Representative T_2-weighted MRI transverse images of (A) untreated, (B) week 2-4 treated, and (C) treated week 3-5 post tumor implantation, at the (left) pre-treatment baseline and weeks (middle) 4 and (right) 5.

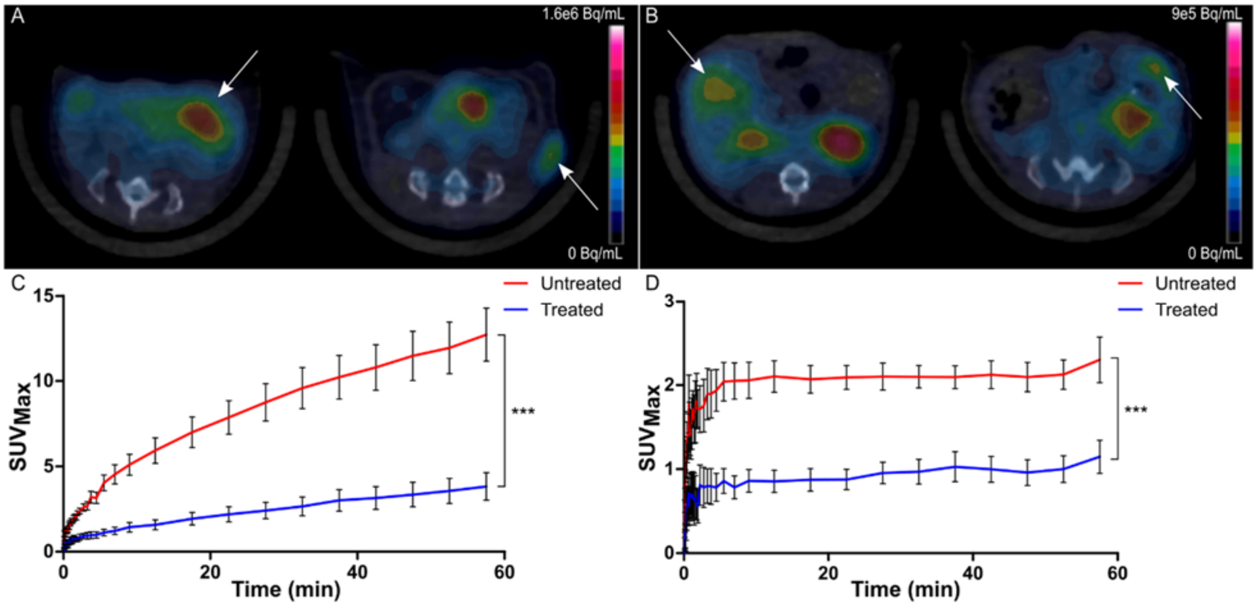

FIGURE 3: Localization of tumor and average time activity profile in treated and untreated 5TGM1 tumor-bearing C57Bl/KaLwRij mice imaged with ^{18}F-FDG and ^{18}F-FDOPA PET/CT. Representative co-registered PET/CT transverse view of (left) untreated and (right) treated tumors in dynamic (A) ^{18}F-FDG and (B) ^{18}F-FDOPA imaging. TACs from (C) ^{18}F-FDG and (D) ^{18}F-FDOPA are displayed (mean ± SEM at each time point), with statistical significance calculated using the 2-way ANOVA with repeated measures (*** $p < 0.001$).

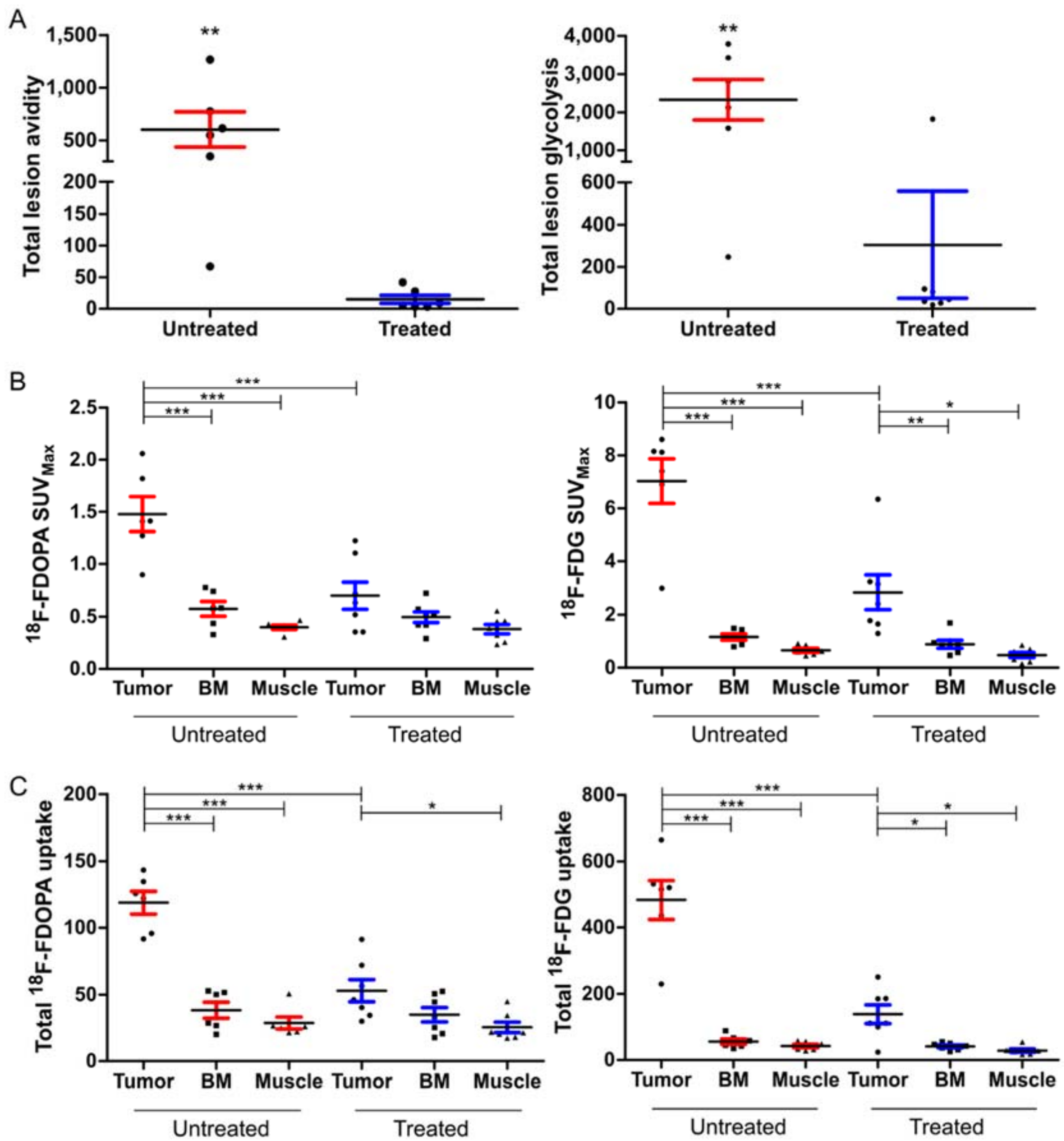

FIGURE 4: Distribution of ^{18}F-FDG and ^{18}F-FDOPA uptake and avidity metrics in treated and untreated 5TGM1 tumor-bearing C57Bl/KaLwRij mice. Scatter plots with mean and SEM distributions are displayed for (A) TLA (left) and TLG (right), (B) SUV_{Max}, and (C) total uptake for ^{18}F-FDOPA (left) and ^{18}F-FDG (right). Statistical significance between treated and untreated cohorts for TLA and TLG was calculated using the two-tailed Student's *t*-test, while 1-way ANOVA with the Bonferroni multiple comparison post-test was used to assess statistical significance between groups and tissue for SUV_{Max} and total uptake (* $p < 0.05$, ** $p < 0.01$, and *** $p < 0.001$).

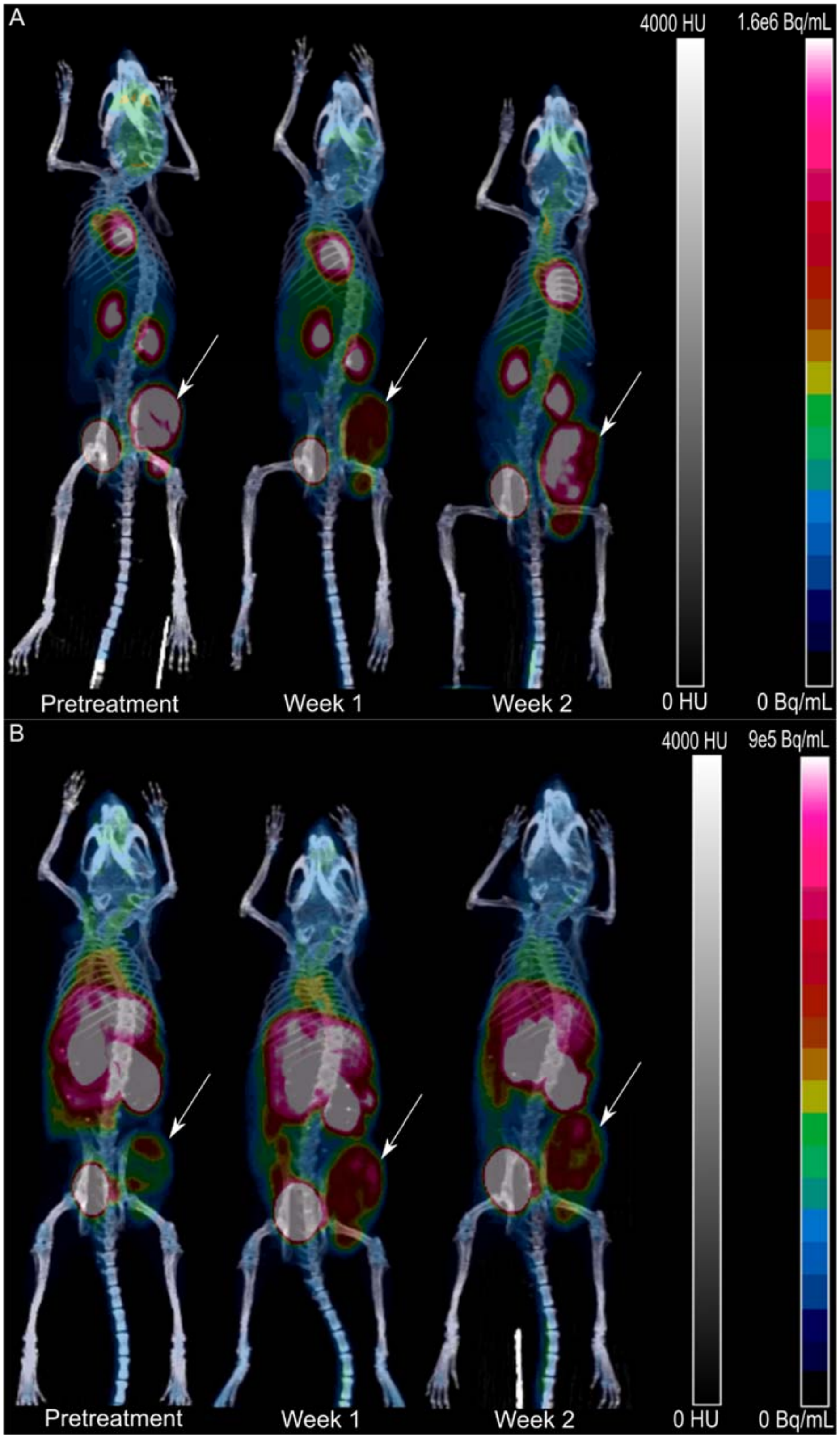

FIGURE 5: Representative maximum intensity projections of longitudinal (A) ^{18}F-FDG and (B) ^{18}F-FDOPA-PET/CT at the pretreated baseline and weeks 1 and 2 during melphalan therapy.

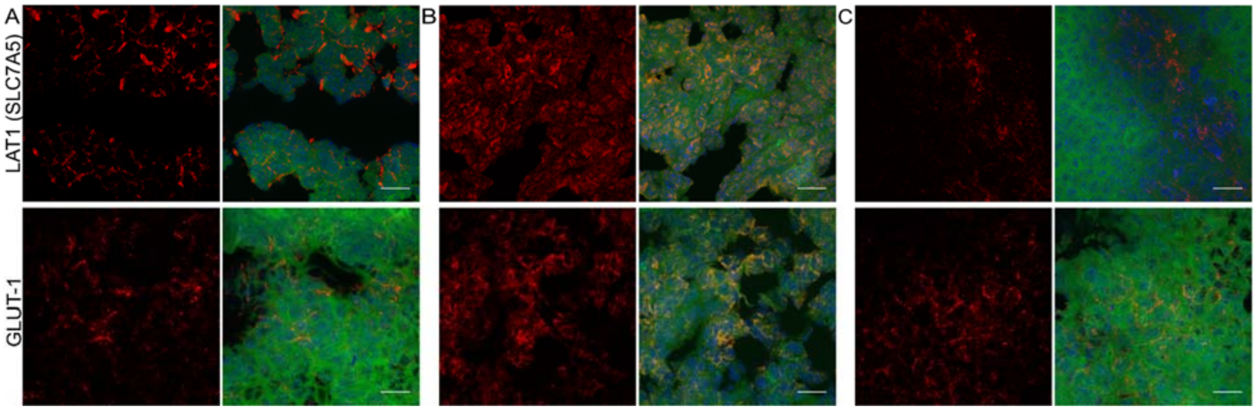

FIGURE 6: Immunohistochemistry of LAT1 (top) and GLUT1 (bottom) expression for (A) untreated and treated tumors with initialization of melphalan therapy at (B) weeks two and (C) three post tumor implantation. Expression for each stain was visualized as a maximum intensity projection (63X magnification; 20μm scale bar) separately and as a composite with GFP (green) and DAPI nuclear stain (blue).

Tables

TABLE 1: Summary of ^{18}F-FDOPA and ^{18}F-FDG measurements

		Treated (n=7) (Mean ± SEM)	Untreated (n=6) (Mean ± SEM)	Untreated : Treated (Mean ± SEM)
Avidity	TLA	13.07 ± 5.89	603.9 ± 165.9	46.21 ± 24.37
	TLG	44.92 ± 12.05	2329 ± 532.1	51.85 ± 18.27
MTV (mm^3)	^{18}F-FDOPA	22.16 ± 7.67	636 ± 194.5	28.7 ± 13.22
	^{18}F-FDG	28.81 ± 5.35	416.1 ± 182.5	14.44 ± 6.88
SUV_{Max}	^{18}F-FDOPA	0.70 ± 0.13	1.48 ± 0.17	2.11 ± 0.46
	^{18}F-FDG	2.84 ± 0.65	7.03 ± 0.84	2.47 ± 0.64
Total Uptake	^{18}F-FDOPA	53.06 ± 8.33	118.9 ± 8.55	2.24 ± 0.39
	^{18}F-FDG	138.8 ± 28.18	483.5 ± 58.98	3.48 ± 0.83
Structural Tumor Volume (mm^3)		78.31 ± 53.6	771.2 ± 291.7	9.85 ± 7.70

TABLE 2: Summary of Lin's correlation coefficients relative to ^{18}F-FDG-PET/CT parameters

	Treated (n=7) Mean (5% - 95% CI)	Untreated (n=6) Mean (5% - 95% CI)
Avidity	0.41 (0.04 – 0.68)	0.16 (-0.08 – 0.4)
MTV	0.64 (-0.01 – 0.91)	0.55 (0.01 – 0.84)
SUV_{Max}	0.03 (-0.11 – 0.16)	0.03 (-0.03 – 0.09)
Total Uptake	0.21 (-0.02 – 0.42)	0.02 (-0.02 – 0.06)

Supplemental Material

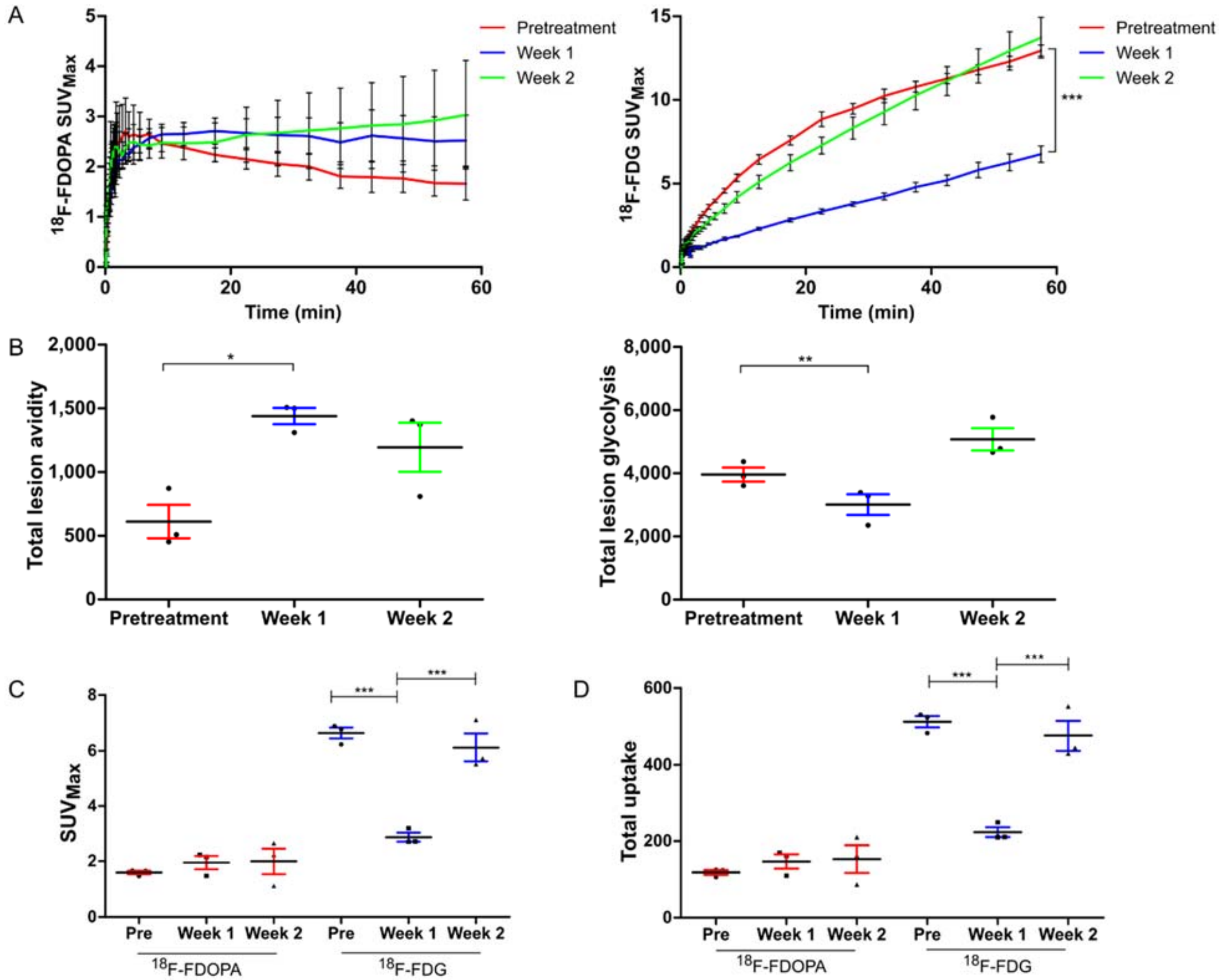

SUPPLEMENTAL FIGURE 1: Distribution of ^{18}F-FDOPA and ^{18}F-FDG uptake metrics during longitudinal treatment and imaging. (A) TACs for ^{18}F-FDOPA (left) and ^{18}F-FDG (right), with statistical significance calculated with 2-way ANOVA with repeated measures and Bonferroni comparisons post-test. (B) TLA (left) and TLG (right) were calculated for each week, as were (C) SUV_{Max} and (D) total uptake from ^{18}F-FDOPA and ^{18}F-FDG TACs. Time points (weeks 1 and 2) were relative to pre-treatment baseline (week 3 post tumor implantation). Statistical significance for the individual comparisons was calculated using 1-way ANOVA with Tukey post-hoc test (**p*<0.05, ***p*<0.01, ****p*<0.001).

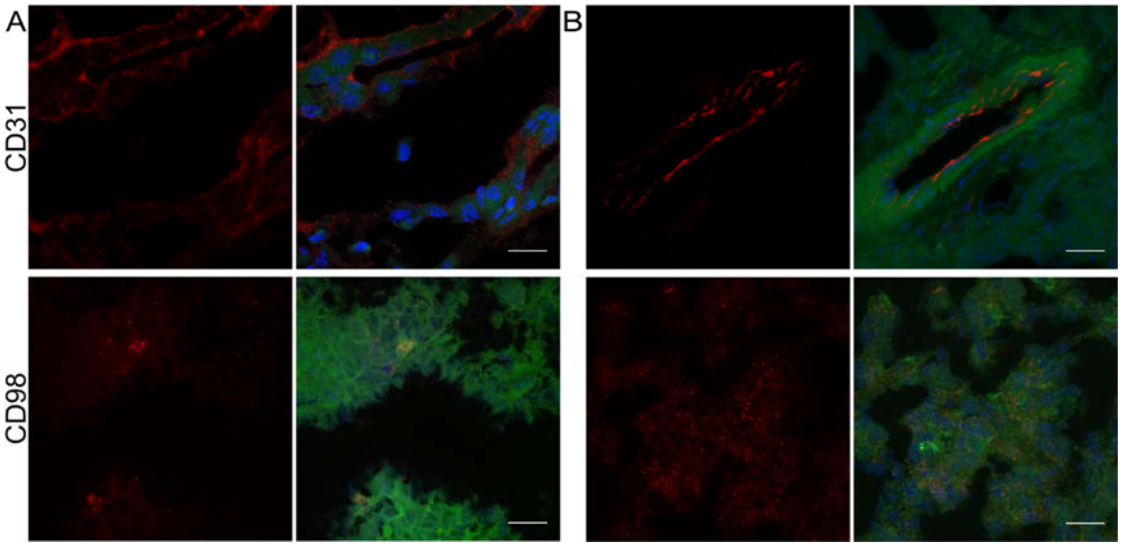

SUPPLEMENTAL FIGURE 2: Immunohistochemistry of CD31 (top) and CD98 (bottom) for representative (A) untreated and (B) treated tumors with initialization of melphalan therapy at week 2 post tumor implantation. Expression for each stain was visualized as a maximum intensity projection (63X magnification; 20μm scale bar) separately and as a composite with GFP (green) and DAPI nuclear stain (blue).